Available online at www.sciencedirect.com
SCIENCE DIRECT
Journal of Power Sources 156 (2006) 677–684
JOURNAL OF POWER SOURCES
www.elsevier.com/locate/jpowsour

Thermodynamic analysis of electrokinetic energy conversion

Xiangchun Xuan, Dongqing Li *

Department of Mechanical and Industrial Engineering, University of Toronto, 5 King's College Road, Toronto, Ont., Canada M5S 3G8

Received 30 April 2005; received in revised form 21 May 2005; accepted 23 May 2005
Available online 11 July 2005

Abstract

A thermodynamic analysis is carried out for electrokinetic energy conversion. We demonstrate that the efficiencies depend solely on the figure of merit Z and are independent of the working mode (generator or pump) at the conditions of maximum power output and maximum efficiency. Between these two extreme points, the ratio of output powers and the ratio of operating conditions (generation voltage or pumping pressure) are also functions of only Z and independent of the working mode. The figure of merit Z associated with phenomenological coefficients is less than one due to the intrinsic entropy production in electrokinetic flows. We establish the phenomenological coefficients through electro-hydrodynamics, and find that Z is dependent on the non-dimensional electrokinetic radius, normalized zeta potential and non-dimensional parameter β characterizing the liquid property. The narrow range of realistic β limits the magnitude of Z to between 0.168 and 0.465 for aqueous solutions. The corresponding maximum efficiency thus varies between 4.59 and 15.51%. Within this range the electrokinetic devices' performance at maximum efficiency is, however, close to that at maximum power output. This feature is identified in a characteristic performance curve of efficiency against output power.

Keywords: Electrokinetic energy conversion; Generator; Pump; Figure of merit; Thermodynamic analysis

1. Introduction

An electrokinetic device can be operated in either a generator or a pump mode. As a generator, a pressure difference is imposed on a liquid in a fine capillary, and an induced streaming current and an induced electrical potential difference (called the streaming potential) are generated between the ends of the capillary, indicating a conversion of mechanical energy into electrical energy (named as the generation power). As a pump, an electrical field is applied across the liquid in a capillary and if the resultant electro-osmotic flow is obstructed, a pressure difference appears indicating a conversion of electrical energy into mechanical energy (named as the pumping power). The streaming potential and electro-osmotic effects were first observed by Reuss [1] in 1809 and Quincke [2] in 1859, respectively. Both effects are associated with electrical double layers forming adjacent to solid–liquid interfaces, which were first proposed by Helmholtz [3] in 1879. After that, several scientists such as Stern and Debye have made great contributions to the double-layer theory and the electrokinetic phenomena (including electrophoresis). A nice overview of this development was presented by Hunter [4].

The pioneering study of electrokinetic energy conversion might owe to Osterle [5] who predicted in 1964 a conversion efficiency of 0.392% with water as the working liquid. Since then, dozens of papers devoted to electrokinetic energy converters have been published. Electrokinetic pumps have received most of the interest because they can generate high pressures and/or high flow rates for chip-based fluid manipulation like microelectronics cooling [6] and chromatographic separation [7]. These pumps are either based on glass columns packed with silica microspheres [8–14] or composed of parallel "slot" structures micro-fabricated in glass [15] and silicon [16] substrates. Santiago and co-workers [17,18] surveyed the progress in the development of microscale electrokinetic pumps. The experimentally measured maximum pumping efficiency is mostly less than 1%, and seems much lower than the theoretically predicted

* Corresponding author. Tel.: +1 416 978 1282; fax: +1 416 978 7753.
E-mail address: dli@mie.utoronto.ca (D. Li).

0378-7753/$ – see front matter © 2005 Elsevier B.V. All rights reserved.
doi:10.1016/j.jpowsour.2005.05.057

Nomenclature

a	capillary radius (m)
e	charge of proton (1.602×10^{-19} C)
E	applied electrical field (V m^{-1})
g_i	defined non-dimensional coefficients, $i = 1, 2, 3$
G	hydrodynamic conductance (m^4 s^{-1} Pa^{-1})
i	electrical current density (A m^{-2})
I	electric current (A)
k_B	Boltzmann's constant (1.3807×10^{-23} JK^{-1})
K	non-dimensional electrokinetic radius
l	capillary length (m)
n_0	bulk ionic density (m^{-3})
M	phenomenological coefficient characterizing the electro-osmotic flow (m^4 V^{-1} s^{-1})
p	hydrodynamic pressure (Pa)
P	applied pressure gradient (Pa m^{-1})
Q	liquid flow rate (m^3 s^{-1})
r	radial coordinate (m)
R	universal gas constant (8.314 J mol^{-1} K^{-1})
S	electrical conductance (Sm)
T	liquid temperature (K)
u	liquid electrokinetic flow velocity (ms^{-1})
W	output power (W)
Z	figure of merit
z_v	valence of ions

Greek letters

β	non-dimensional property of liquid
η	conversion efficiency
ε	dielectric constant of liquid (C V^{-1} m^{-1})
ϕ	electrical potential (V)
Λ	molar conductivity of liquid (m^2 S mol^{-1})
μ	liquid viscosity (K gm^{-1} s^{-1})
ρ_e	net charge density (C m^{-3})
σ_0	electrical conductivity of liquid (S m^{-1})
ψ	electrical double-layer potential (V)
ζ	zeta potential of the capillary surface (V)
ζ^*	non-dimensional zeta potential of the capillary surface

Subscripts

max W	maximum output power
max η	maximum conversion efficiency

efficiency. Without restricting to small surface potentials or thin double-layers, numerically calculated pumping efficiencies could be 10% [19] and 15% [20] in a cylindrical capillary at the conditions of maximum pumping power and maximum pumping efficiency, respectively.

Only a few of past papers have investigated electrokinetic generators. Forty years ago Burgreen and Nakache [21] predicted an efficiency of approximately 17% for a generator using water in equilibrium with the CO_2 in the air. However, the maximum efficiency of a recently developed electrokinetic microchannel battery using tap water is barely on the order of 0.01% [22]. More recently, Daiguji et al. [23] investigated the electro-chemo-mechanical energy conversion in nanofluidic channels and predicted an efficiency of more than 1%. Another discovery is a voltage induced by a liquid flow in carbon nanotube bundles [24]. While the underlying mechanism is still unclear [25,26], this phenomenon explores the potential of energy conversion in nanotubes.

In analyzing the efficiency of electrokinetic energy conversion, the great majority of previous studies employed directly the theory of electrokinetic microchannel flow. As numerical solutions were necessarily involved in these analyses, however, the true factors affecting the devices performance were missed or left behind the complex formulae. In essence, electrokinetic devices utilize the liquid flow and electrical current to realize the thermodynamic conversion between mechanical energy and electrical energy. Therefore, we turn to a thermodynamic analysis of electrokinetic energy conversion in this paper, and provide a new understanding of devices performance at the conditions of maximum power output and maximum efficiency. We noticed that Osterle and co-workers had employed the phenomenological equations to investigate the electrokinetic energy conversion [27,28]. However, they focused mainly on the maximum conversion efficiency, and ignored the performance at the maximum power output. Therefore, the comparison of device performance and operating conditions at the two extreme points is still lacking from the thermodynamic viewpoint. Moreover, the parametric study of conversion efficiency and output power is incomplete from the electrokinetic viewpoint.

This paper is organized as follows. In Section 2 a thermodynamic analysis is presented for irreversible electrokinetic energy conversion process. The operating conditions and devices performance at maximum power output and maximum efficiency are derived in terms of phenomenological coefficients, and an important parameter Z, named as figure of merit, is defined. In Section 3 the phenomenological coefficients and also Z are specified through electro-hydrodynamics. We examine in Section 4 the factors affecting Z and thus the performance of a practical electrokinetic generator as an example. A summary of our results and a few technical comments are provided in Section 5.

2. Thermodynamic analysis

Within the linear response regime of electrokinetic flow, the Onsager reciprocal theorem relates the liquid flow rate Q and the electrical current I though a capillary (of any cross-sectional shape), to the pressure difference Δp and the electrical potential difference $\Delta\phi$ between its entrance and

exit [29,30]:

$$Q = G(-\Delta p) + M(-\Delta\phi) \tag{1}$$

$$I = M(-\Delta p) + S(-\Delta\phi) \tag{2}$$

where G represents the hydrodynamic conductance, M characterizes the electro-osmotic flow in Eq. (1) and the streaming current in Eq. (2), and S indicates the electrical conductance. It is noted that in the generation mode, the pressure decreases in the direction of fluid flow (to provide mechanical power) and the voltage increases in the direction of current (acting as a battery). In the pumping mode, however, the pressure increases in the direction of fluid flow and the voltage decreases in the direction of current (to provide electrical power). As such, the output power W and the conversion efficiency η are, respectively, given by:

$$W = I\Delta\phi \quad \text{for generators, and} \quad W = Q\Delta p \quad \text{for pumps} \tag{3}$$

$$\eta = \frac{I\Delta\phi}{Q(-\Delta p)} \text{for generators, and} \quad \eta = \frac{Q\Delta p}{I(-\Delta\phi)} \text{for pumps.} \tag{4}$$

Substituting Q and I in Eqs. (3) and (4) with the expressions in Eqs. (1) and (2) yields W and η that are both functions of solely the generation voltage $\Delta\phi$ for generators (where a known pressure difference Δp is applied)) or the pumping pressure Δp for pumps (where a known potential difference $\Delta\phi$ is applied). Therefore, we can maximize W and η separately by differentiating them with respect to either $\Delta\phi$ or Δp. This mathematical manipulation is straightforward and hence omitted here. The resultant performance formulae are summarized below.

2.1. Maximum generation power or pumping power

For electrokinetic generators, the generation power is maximized when the generation voltage achieves:

$$\Delta\phi_{\max W} = \frac{M}{2S}(-\Delta p) \tag{5}$$

where the subscript max W signifies the condition of maximum generation power (or the maximum pumping power for liquid pumps presented later). Note that $\Delta\phi_{\max W}$ in Eq. (5) is exactly half of the maximum voltage produced by the generator, when the electrical current I in Eq. (2) vanishes and hence W and η are both zero. The maximum generation power and the corresponding conversion efficiency are given by:

$$W_{\max W} = \frac{1}{4}ZG(\Delta p)^2 \tag{6}$$

$$\eta_{\max W} = \frac{Z}{2(2-Z)} \tag{7}$$

$$Z = \frac{M^2}{GS}. \tag{8}$$

One can see that $\eta_{\max W}$ is solely dependent on the non-dimensional parameter Z that is less than 1 according to Prigogine's theorem [31]. Within this limit, $\eta_{\max W}$ is a monotonically increasing function of Z and we shall call it the "figure of merit" following Osterle and co-workers [27,28]. In fact, this figure of merit Z can be viewed as the product of the streaming current effect in Eq. (9) and the electro-osmotic effect in Eq. (10) (refer to Eqs. (1) and (2)) [29,31]:

$$\frac{M}{G} = \left(\frac{I}{Q}\right)_{\Delta\phi=0} \tag{9}$$

$$\frac{M}{S} = \left(\frac{Q}{I}\right)_{\Delta p=0}. \tag{10}$$

These two effects occurring simultaneously in electrokinetic devices underlie the energy conversion principle of electrokinetic generators and pumps. The significance of the figure of merit Z will be explored in the next section.

In the pumping mode, the maximum pumping power and the corresponding pumping pressure are expressed as:

$$W_{\max W} = \frac{1}{4}ZS(\Delta\phi)^2 \tag{11}$$

$$\Delta p_{\max W} = \frac{M}{2G}(-\Delta\phi). \tag{12}$$

As this condition, however, the pumping efficiency is identical to the generation efficiency in Eq. (7).

2.2. Maximum generation efficiency or pumping efficiency

For electrokinetic generators, the conversion efficiency is maximized when the generation voltage satisfies:

$$\Delta\phi_{\max\eta} = \frac{G}{M}(1-\sqrt{1-Z})(-\Delta\phi) \tag{13}$$

where the subscript max η indicates the condition of maximum generation or pumping efficiency. At this condition, the generation power and efficiency are given by:

$$W_{\max\eta} = G\frac{\sqrt{1-Z}(1-\sqrt{1-Z})^2}{Z}(\Delta p)^2 \tag{14}$$

$$\eta_{\max\eta} = \frac{(1-\sqrt{1-Z})^2}{Z}. \tag{15}$$

Eq. (15) also applies to the maximum pumping efficiency when the pumping pressure reaches:

$$\Delta p_{\max\eta} = \frac{S}{M}(1-\sqrt{1-Z})(-\Delta\phi). \tag{16}$$

The corresponding pumping power is described by:

$$W_{\max\eta} = S\frac{\sqrt{1-Z}(1-\sqrt{1-Z})^2}{Z}(\Delta\phi)^2. \tag{17}$$

Osterle [5] first proved that the efficiency of electrokinetic energy converters is independent of the working mode, which

is attributed to the Onsager reciprocal relation (see Eqs. (1) and (2)). Evidently the maximum generation or pumping efficiency in Eq. (15) is also a monotonically increasing function of the figure of merit Z. Moreover, we notice that both the ratio of output powers, Eq. (18), and the ratio of operating conditions, Eq. (19), between the two extreme points discussed above are also functions of solely Z and independent of the working mode:

$$\frac{W_{\max W}}{W_{\max \eta}} = \frac{(1+\sqrt{1-Z})^2}{4\sqrt{1-Z}} \tag{18}$$

$$\frac{\Delta p_{\max W}}{\Delta p_{\max \eta}} = \frac{\Delta \phi_{\max W}}{\Delta \phi_{\max \eta}} = \frac{1+\sqrt{1-Z}}{2}. \tag{19}$$

As seen from these two equations, the figure of merit Z gauges the performance of electrokinetic energy converters. The ultimate goal of electrokinetic devices researchers is to maximize Z in Eq. (8), which can be realized by improving the streaming current effect in Eq. (9) and/or the electro-osmotic effect in Eq. (10). This issue will be addressed later in this paper.

Fig. 1 compares the efficiencies under the conditions of maximum output power and maximum efficiency. As stated previously, both efficiencies increase with the rise of Z. However, only at $Z \geq 0.6$ can these two efficiencies be distinguished (5% difference). In the high Z limit (i.e., $Z \to 1$), $\eta_{\max W}$ achieves 0.5 while $\eta_{\max \eta}$ approaches 1. We will demonstrate later in this paper that the realistic Z is outside of this region. Therefore, the above two extreme conditions are essentially close to each other in typical electrokinetic energy converters. The two ratios defined in Eqs. (18) and (19) are demonstrated in Fig. 2 against different values of Z. The discrepancy in the output powers at the two extremes is again less than 5% unless $Z \geq 0.6$. However, the operating conditions, say generation voltage, are significantly different provided that $Z \geq 0.2$. The magnitude of generation voltage (or pumping pressure, not shown in the axis label of right ordinate) at the condition of maximum output power is always

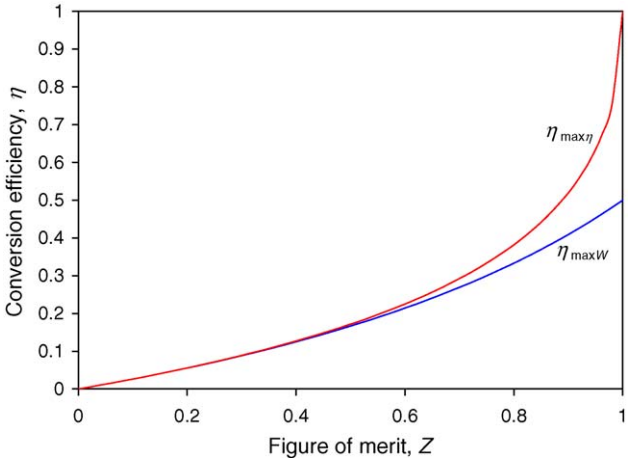

Fig. 1. Efficiencies vs. the figure of merit Z under conditions of maximum output power and maximum conversion efficiency for electrokinetic energy converters.

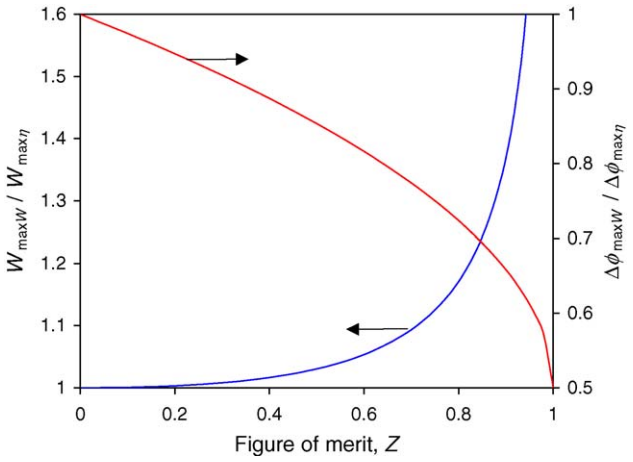

Fig. 2. Ratios of output power and generation voltage for generators (or pumping pressure for pumps) vs. the figure of merit Z between the conditions of maximum output power and maximum conversion efficiency.

lower than that at maximum efficiency. In the high Z limit (i.e., $Z \to 1$), the former is only half of the latter. Note that $\eta_{\max W}$ is also half of $\eta_{\max \eta}$ in this limit.

3. Mathematical formulation

We have demonstrated in the preceding section that the electrokinetic devices performance is associated with the coefficients G, M and S in the phenomenological Eqs. (1) and (2). In this section, we want to specify these coefficients through the electrokinetic flow theory for the capillary model, i.e., a cylindrical tube of length l and radius a. However, the same method presented here also applies to channels of other cross-sectional shapes such as slit or rectangular channels. It is well known that the liquid electrokinetic flow velocity u consists of electro-osmotic flow (the first term on the right hand side of Eq. (20)) and pressure-driven flow (the second hand on the right hand side of Eq. (20)) [32]:

$$u = -\frac{\varepsilon\zeta}{\mu}\left(\frac{\psi}{\zeta}-1\right)\frac{\Delta\phi}{l} - \frac{a^2}{4\mu}\left(1-\frac{r^2}{a^2}\right)\frac{\Delta p}{l} \tag{20}$$

where ε is dielectric constant of the liquid, μ the liquid viscosity, r the radial coordinate, ψ the electrical double-layer potential induced by the surface charge at the channel wall that is often characterized by the zeta potential ζ. Neglecting the diffusive ion fluxes in the direction of the applied electrical field and assuming a Boltzmann distribution of ions, the local current density i in a symmetric electrolyte is given by [4,19,20]:

$$i = \sigma_0 \cosh(z_v e\psi/k_B T)\frac{-\Delta\phi}{l} + \rho_e u \tag{21}$$

where σ_0 is the electrical conductivity of the bulk liquid, z_v the valence of ions, e the charge of proton, k_B the Boltzmann's constant, T the liquid temperature, and ρ_e the net

charge density that is determined from the Poisson equation:

$$\rho_e = -\varepsilon \nabla^2 \psi. \tag{22}$$

Integrating Eqs. (20) and (21) over the channel cross-section and comparing with the phenomenological Eqs. (1) and (2) yield [33]:

$$G = \frac{\pi a^4}{8\mu l} \tag{23}$$

$$M = -\frac{\pi \varepsilon a^2 \zeta}{\mu l} g_1 \tag{24}$$

$$S = \frac{\pi \varepsilon^2 \zeta^2}{\mu l}(g_2 + \beta g_3) \tag{25}$$

$$g_1 = 1 - 2\int_0^a \left(\frac{r}{a}\right)\left(\frac{\psi}{\zeta}\right) \mathrm{d}\left(\frac{r}{a}\right) \tag{26}$$

$$g_2 = 2\int_0^a \left(\frac{r}{a}\right)\left[\frac{\mathrm{d}(\psi/\zeta)}{\mathrm{d}(r/a)}\right]^2 \mathrm{d}\left(\frac{r}{a}\right) \tag{27}$$

$$g_3 = \frac{K^2}{\zeta^{*2}}\int_0^a \left(\frac{r}{a}\right) \cosh\left(\frac{ze\psi}{k_B T}\right) \mathrm{d}\left(\frac{r}{a}\right) \tag{28}$$

It is noted that g_i defined in Eqs. (26)–(28) are all positive and independent of the sign of zeta potential. In these equations, the distribution of double-layer potential ψ is solved from the Poisson–Boltzmann equation [4]:

$$\nabla^2 \psi = \frac{2 z_v e n_0}{\varepsilon} \sinh\left(\frac{z_v e \psi}{k_B T}\right) \tag{29}$$

where n_0 is the bulk ionic density. To this end, the figure of merit Z in Eq. (8) can be specified as:

$$Z = \frac{8 g_1^2}{g_2 + \beta g_3}. \tag{30}$$

There appear three important non-dimensional parameters in the definition of Z in Eq. (30). The first one β is the ratio of the conductive current, Λ in Eq. (31), to the convective current due to electro-osmosis, ε/μ in Eq. (31), and essentially characterizes a non-dimensional property of the working liquid[1]:

$$\beta = \frac{\Lambda \mu}{\varepsilon R T} \tag{31}$$

where Λ is the molar conductivity, and R the universal gas constant. As g_i in the definition of the figure of merit Z, Eq. (30), are positive, a smaller β is desirable in order to attain a higher Z. Since Λ varies only between about 4 and 20 mS m^2 mol^{-1} for aqueous solutions [34], however, the realistic values of β likely span the small range $2 < \beta < 10$. We will demonstrate in the next section that it is mainly this small range of β that limits the magnitude of Z. The other two parameters that hide in the definitions of g_i (see Eqs. (26)–(28)) are the non-dimensional electrokinetic radius:

$$K = a\sqrt{\frac{2 z_v^2 e^2 n_0}{\varepsilon k_B T}} \tag{32}$$

and the normalized zeta potential:

$$\zeta^* = \frac{e\zeta}{k_B T}. \tag{33}$$

Up to this point, the phenomenological coefficients and the figure of merit Z have been determined. The only problem remaining to be solved is the distribution of double-layer potential in Eq. (29), which will be addressed in the proceeding section.

4. Results and discussion

To examine the effects of the three non-dimensional parameters β, K and ζ^* on electrokinetic devices performance, we first need to determine the double-layer potential ψ. Here, Eq. (29) was analytically solved with the method proposed by Levine et al. [35] that is applicable to cylindrical channels with arbitrary zeta potential and arbitrary non-dimensional electrokinetic radius. The integrations involved in Eqs. (26)–(28) were numerically evaluated with Simpson's rule.

Fig. 3 shows a characteristic performance curve, i.e., efficiency η against output power W, of an electrokinetic generator working with pure water (of 10^{-5} M ionic concentration). The generation power has been normalized by its maximum value $W_{\max W}$. The capillary radius is $a = 0.2$ μm. Other necessary parameters are [34]:

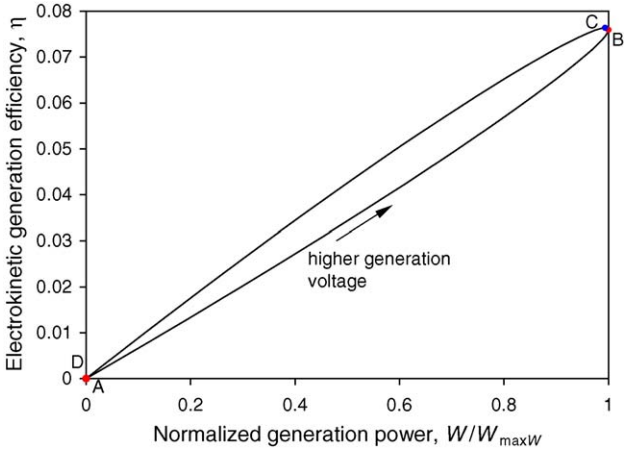

Fig. 3. Characteristic performance curve of electrokinetic generators. The generation power is normalized by its maximum value. The curve vanishes in the limits of low (A) and high (D) generation voltage due to the vanishing voltage and the vanishing electrical current, respectively. The two adjacent points are maximum generation power (B) and maximum generation efficiency (C). Pure water (of 10^{-5} M concentration) is the working liquid, and the capillary radius is 0.2 μm. All other parameters are referred to the text.

[1] In Griffiths and Nilson's paper [19], the reciprocal of β is named as Levine number.

viscosity $\mu = 0.9 \times 10^{-3}$ K gm^{-1} s^{-1}, relative dielectric constant $\varepsilon = 80 \times 8.854 \times 10^{-12}$ C V^{-1} m^{-1}, molar conductivity $\Lambda = 10$ m S m^2 mol^{-1}, zeta potential $\zeta = -100$ mV, and room temperature $T = 298$ K. The resultant figure of merit Z is 0.264 where the involved non-dimensional parameter β is 5.128. The four points noted on the curve are: (1) A represents the vanishing efficiency in the low-generation voltage limit; (2) B represents the maximum generation power; (3) C represents the maximum generation efficiency; (4) D represents the vanishing efficiency in the high-generation voltage limit. The points A and D collapse to the origin because either the generation voltage (at point A) or the electrical current (at point D) is zero so that the generation power vanishes. The two extreme points B and C are close to each other because the figure of merit Z under investigation is small (refer to Fig. 1).

We are interested in the likely magnitude of Z when β is within the practical range of $2 < \beta < 10$ for typically used aqueous solutions. Fig. 4 shows the contours of Z as a function of the non-dimensional electrokinetic radius K and the normalized zeta potential ζ^* at $\beta = 2$ (top) and $\beta = 10$ (bottom), respectively. In this range of β, the highest magnitude of Z varies only between 0.465 (top) and 0.168 (bottom), within which the performances at the conditions of maximum power output and maximum efficiency are essentially indistinguishable (refer to Fig. 1). Interestingly and importantly, Z achieves its summit in a range of K and ζ^*, not a particular set of these two parameters. For example at $\beta = 10$ (bottom subfigure in Fig. 4), Z remains nearly constant at $\zeta^* \geq 4$ despite that K drifts toward lower values as ζ^* grows larger. In other words, it is unnecessary to choose extremely high zeta potentials and/or extremely small pores. This prediction is consistent with those from Griffiths and Nilson [19] and Min et al. [20], who analyzed the performances at maximum pumping power and maximum pumping efficiency, respectively. We also notice that as β decreases, the lower limit of ζ^* that optimizes Z becomes smaller while the corresponding K remains almost unchanged.

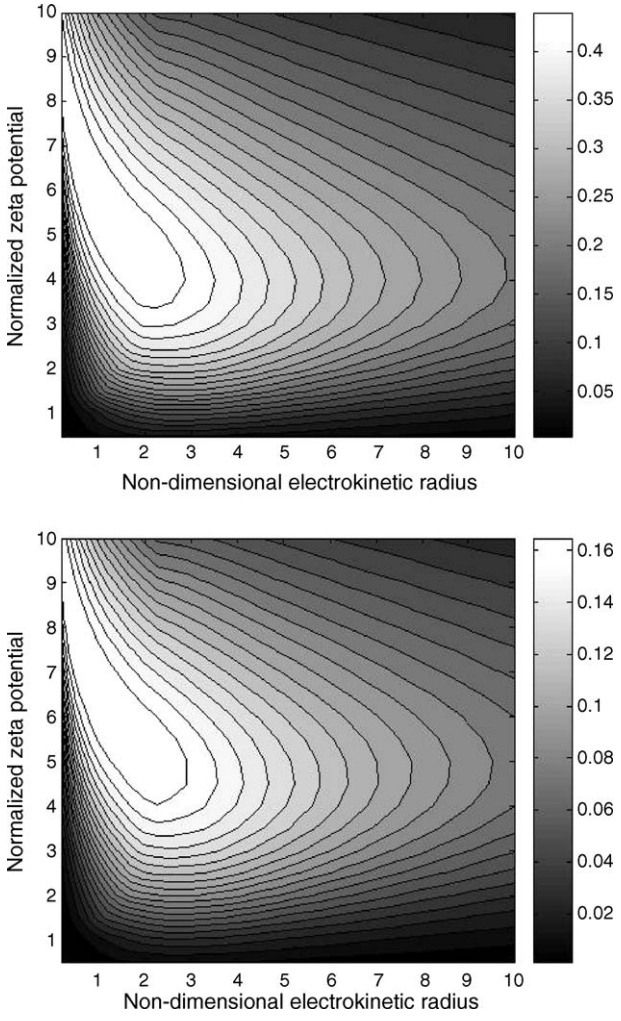

Fig. 4. The contours of figure of merit Z as a function of the non-dimensional electrokinetic radius K and the normalized zeta potential ζ^* at $\beta = 2$ (top) and $\beta = 10$ (bottom). The highest magnitudes of Z are, respectively, 0.465 (top) and 0.168 (bottom).

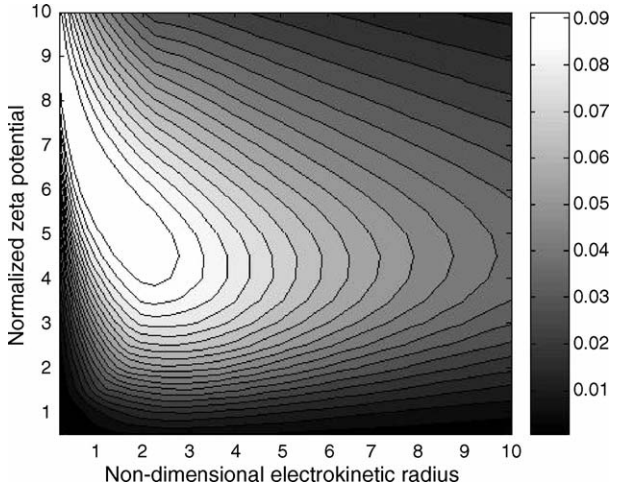

Fig. 5. The contours of maximum generation efficiency $\eta_{\max \eta}$ as a function of the non-dimensional electrokinetic radius K and the normalized zeta potential ζ^* at $\beta = 4$. The highest magnitude of $\eta_{\max \eta}$ is 9.66%.

As the generation or pumping efficiencies at the two extreme conditions increase with the rise of the figure of merit Z (see Fig. 1), they should follow the same pattern as Z increases with K and ζ^*. Fig. 5 shows the contour of maximum conversion efficiency at $\beta = 4$, which is quite similar to the efficiency contour at the condition of maximum output power (not shown). By choosing optimum values of K and ζ^*, we can get an efficiency of 9.66% at most. If $\beta = 2$ is assumed, instead, the maximum efficiency could go as high as 15.51%. This efficiency in close agreement with Min et al. [20] analysis is much higher than the best experimental efficiency reported to date [18]. It turns out that β is the determinant factor in the electrokinetic conversion efficiency. Therefore, more attention should be paid to the search of electrolyte solution with a high β in the future. For example, Kirby and co-workers [36,37] have recently demonstrated the performance improvement of electrokinetic micropumps by using zwitterionic solute additives.

Other than the figure of merit Z, the output powers under the conditions of maximum power output and maximum conversion efficiency are also related to the liquid conductance (specifically, hydrodynamic conductance for generators and electrical conductance for pumps, see Eqs. (6), (11), (14) and (17)). However, these two powers are approximately the same in realistic electrokinetic devices due to the small magnitude of Z. Hence, we investigate only the maximum generation power in Eq. (6) and the maximum pumping power in Eq. (11) that are specified as:

$$\frac{W_{\max W}}{l} = ZP^2\frac{\pi a^4}{32\mu} \quad \text{for generators, and} \quad \frac{W_{\max W}}{l} = \frac{2\pi\varepsilon^2 E^2}{\mu}\zeta^2 g_1^2 \quad \text{for pumps} \tag{34}$$

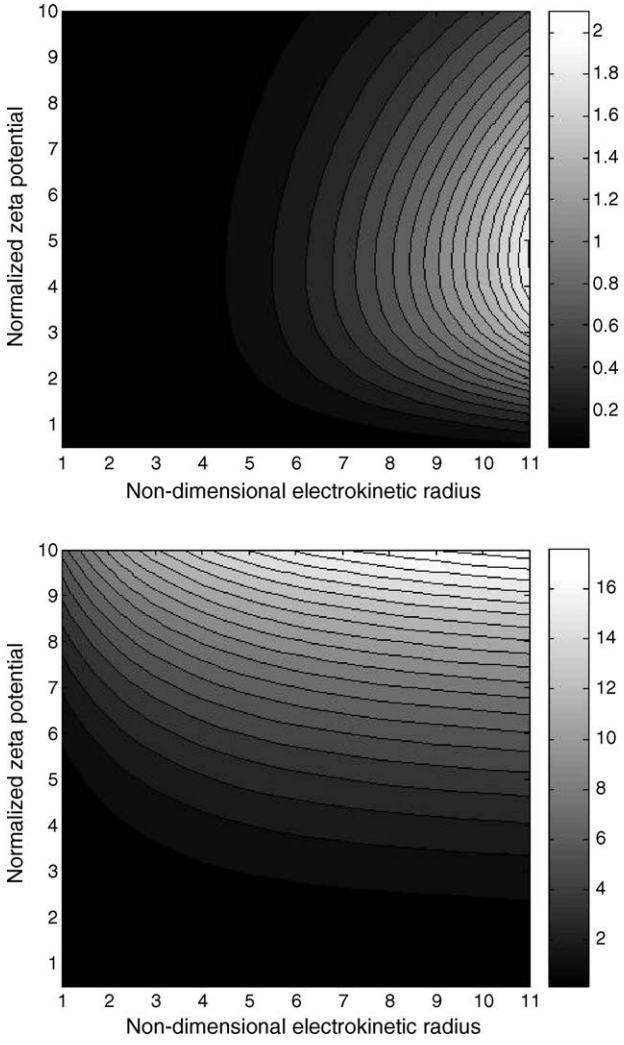

Fig. 6. The contours of maximum generation power (top) and maximum pumping power (bottom) as a function of the non-dimensional electrokinetic radius K and the normalized zeta potential ζ^* at $\beta = 4$. The applied pressure gradient is $P = 1$ atm cm^{-1} for the generator and the applied electrical field is $E = 100$ V cm^{-1} for the pump. The unit for the contour bar is nW m^{-1} for both cases.

where $P = -\Delta p/l$ and $E = -\Delta\phi/l$ denote the applied pressure gradient and electrical field, respectively. One can see that the maximum generation power is a strong function of capillary radius and thus a larger pore is desirable as well as a higher figure of merit Z. The maximum pumping power is, however, not directly dependent on Z and thus not limited by the non-dimensional liquid property β. Yao and Santiago [17] have demonstrated numerically that g_1 (see Eq. (26)) increases with the rise of non-dimensional electrokinetic radius K. Also, g_1 is only a weak function of zeta potential ζ (or ζ^*). Therefore, the maximum pumping power is enhanced when K and/or ζ^* become larger. Fig. 6 shows the contours of maximum generation power (top) and maximum pumping power (bottom) at $\beta = 4$. The applied pressure gradient for the generator is $P = 1$ atm cm^{-1}, and the applied electrical field for the pump is $E = 100$ V cm^{-1}. As expected, both powers increase with the rise of non-dimensional electrokinetic radius K (i.e., capillary radius). As the maximum generation power (top) is proportional to Z, it follows the similar trend to Fig. 4 against the normalized zeta potential ζ^*. For liquid pumps, however, the maximum pumping power is elevated at higher ζ^*.

5. Conclusions

Based on the general Onsager relation in electrokinetic flow, we have conducted a thermodynamic analysis for electrokinetic generators and pumps. Their conversion efficiencies at the condition of maximum power output and the condition of maximum efficiency are exactly the same. These two efficiencies depend solely on the figure of merit Z. This Z also governs the ratio of output powers and the ratio of operating conditions (i.e., generation voltage or pumping pressure) between the two extreme points. Moreover, these two ratios are independent of the working mode. The figure of merit Z expressed by the phenomenological coefficients is less than 1 due to the intrinsic entropy production in irreversible electrokinetic flows. In the high limit of Z, the maximum efficiency approaches 1 with zero power output while the efficiency at maximum power output achieves 0.5. In the same limit, the generation voltage or pumping pressure at maximum power output is reduced to half of that at maximum efficiency.

We have also determined the phenomenological coefficients and thus the figure of merit Z through electro-hydrodynamic analysis. We find that Z is dependent on non-dimensional electrokinetic radius K, normalized zeta potential ζ^* and non-dimensional liquid property β. This β, the ratio of conductive current to convective current due to electro-osmosis, spans the small range $2 < \beta < 10$ for aqueous solutions. As a result, the optimal Z calculated numerically varies only between 0.465 and 0.168. The corresponding maximum efficiency varies between 4.59 and 15.51%. The latter value is much higher than the best experimentally reported efficiency of 5.6% [36], indicating a potentially large developing space for

state-of-the-art electrokinetic pumps. We also find that the practically small Z has dimmed the performance difference at maximum power output and maximum efficiency. This feature has been demonstrated in the performance curve of efficiency against power output for an electrokinetic generator working with pure water. In addition, our analysis suggests that future work on electrokinetic energy converters should be focused on the search of electrolytes with a high β.

Acknowledgement

Financial support from the Natural Sciences and Engineering Research Council (NSERC) of Canada, through a research grant to D. Li is gratefully acknowledged.

References

[1] F.F. Reuss, Mem. Soc. Imp. Naturalistes Moscow 2 (1809) 327.
[2] G. Quincke, Pogg. Ann. Phys. 107 (1859) 1.
[3] H.L.F. Helmholtz, Wied. Ann. 7 (1879) 337.
[4] R.J. Hunter, Zeta Potential in Colloid Science, Principals and Applications, Academic Press, New York, 1981.
[5] J.F. Osterle, J. Appl. Mech. 31 (1964) 161.
[6] L. Jang, J. Mikkelsen, J. Koo, D. Huber, S. Yao, L. Zhang, P. Zhou, J.G. Maveety, R. Prasher, J.G. Santiago, T.W. Kenny, K.E. Goodson, IEEE Trans. Compon. Pack. Technol. 25 (2002) 347.
[7] J.E. MacNair, K.C. Lewis, J.W. Jorgenson, Anal. Chem. 69 (1997) 983.
[8] V. Pretorius, B.J. Hopkins, J.D. Schieke, J. Chromatogr. A 99 (1974) 23.
[9] F. Theeuwes, J. Pharmaceut. Sci. 12 (1975) 1987.
[10] P.H. Paul, D.W. Arnold, D.J. Rakestraw, Proceedings of the μTAS 98, Banff, Canada, 1998.
[11] S. Zeng, C. Chen, J.C. Mikkelsen, J.G. Santiago, Sens. Actuators B 79 (2001) 107.
[12] S. Zeng, C. Chen, J.C. Mikkelsen, J.G. Santiago, J.R. Chen, R.N. Zare, J.A. Tripp, F. Svec, J.M.J. Fréchet, Sens. Actuators B 82 (2002) 209.
[13] J.A. Tripp, F. Svec, J.M.J. Fréchet, S. Zeng, J.C. Mikkelsen, J.G. Santiago, Sens. Actuators B 99 (2004) 66.
[14] S. Yao, D.E. Hertzog, S. Zeng, J.C. Mikkelsen, J.G. Santiago, J. Colloid Interf. Sci. 268 (2004) 143.
[15] C. Chen, J.G. Santiago, J. Microelectromech. Syst. 11 (2002) 672.
[16] D.J. Laser, S. Yao, C. Chen, J.C. Mikkelsen, K.E. Goodson, J.G. Santiago, T. Kenny, Proceedings of the Transducers '01, Munich, 2001.
[17] S. Yao, J.G. Santiago, J. Colloid Interf. Sci. 268 (2004) 133.
[18] D.J. Laser, J.G. Santiago, J. Micromech. Microeng. 14 (2004) R35.
[19] S.K. Griffiths, R.H. Nilson, Electrophoresis 26 (2005) 351.
[20] J.Y. Min, E.F. Hasselbrink, S.J. Kim, Sens. Actuators B 98 (2004) 368.
[21] D. Burgreen, F.R. Nakache, J. Appl. Mech. 32 (1965) 675.
[22] J. Yang, F. Lu, L.W. Kostiuk, D.Y. Kwok, J. Micromech. Microeng. 13 (2003) 963.
[23] H. Daiguji, P. Yang, A.J. Szeri, A. Majumdar, Nano Lett. 4 (2004) 2315.
[24] S. Ghosh, A.K. Sood, N. Kumar, Science 299 (2003) 1042.
[25] E. Cohen, Science 300 (2003) 1235.
[26] S. Ghosh, A.K. Sood, N. Kumar, Science 300 (2003) 1235.
[27] F.A. Morrison, J.F. Osterle, J. Chem. Phys. 43 (1965) 2111.
[28] R.J. Gross, J.F. Osterle, J. Chem. Phys. 49 (1968) 228.
[29] S.R. de Groot, P. Mazur, Non-Equilibrium Thermodynamics, North-Holland, Amsterdam, 1969.
[30] E. Brunet, A. Ajdari, Phys. Rev. E 69 (2004) 016306.
[31] I. Prigogone, Introduction to Thermodynamics of Irreversible Processes, Interscience Publishers, 1968.
[32] D. Li, Electrokinetics in Microfluidics, Elsevier Academic Press, Burlington, MA, 2004.
[33] X. Xuan, D. Li, J. Micromech. Microeng. 14 (2004) 290.
[34] R.F. Probstein, Physicochemcial Hydrodynamics, Wiley, New York, 1995.
[35] S. Levine, J.R. Marriott, G. Neale, N. Epstein, J. Colloid Interf. Sci. 52 (1975) 136.
[36] D.S. Reichmuth, G.S. Chirica, B.J. Kirby, Sens. Actuators B 92 (2003) 37.
[37] D.S. Reichmuth, B.J. Kirby, J. Chromatogr. A 1013 (2003) 93.